Desalination and Water Treatment
www.deswater.com

doi: 10.1080/19443994.2015.1136965

57 (2016) 23644–23650
October

Taylor & Francis
Taylor & Francis Group

Investigation of photocatalytic performance of TiO_2 network and fiber geometries

Hassan Koohestani[a,*], Sayed Khatiboleslam Sadrnezhaad[b], Amirabbas Kheilnejad[c]

[a]*Faculty of Materials and Metallurgical Engineering, Semnan University, Semnan, Iran, Tel. +98 23 33654100; Fax: +98 23 33321005; email: h_koohestani@seman.ac.ir*
[b]*Department of Materials Science and Engineering, Sharif University of Technology, Azadi Ave., Tehran, Iran, Tel. +98 21 66161; email: sadrnezh@yahoo.com*
[c]*Instructor Training Center and Technical and Vocational Researches, University of Applied Sciences and Technology, Tehran, Iran, email: a.kheilnejad@gmail.com*

Received 17 July 2015; Accepted 23 December 2015

ABSTRACT

In typical photocatalytic processes slurry reactors are used in which catalyst particles have to be separated from the solution after the process ends which means much higher time and costs. Hence, immobilizing process is carried out on the catalyst to overcome this problem. In this work, fiber and network geometries were produced by particle precipitation on substrates. The obtained structures were characterized by XRD, SEM, and Brunauer–Emmett–Teller analyses. Photocatalytic performance of the samples was investigated by methyl orange degradation and also by hydrogen generation from water/methanol splitting. From the SEM images, the size range of the TiO_2 particles in the network geometries were 20–60 nm. The nanoparticles had covered the surface of the substrate uniformly. Removal of the cellulose substrate by heat treatment yielded hollow TiO_2 fibers with diameters of 0.5–1 μm and lengths of 30 μm. The rate constant of the dye degradation reaction using powder catalyst was 0.0118 min^{-1}. However, the rate constants for fiber and network geometries were 0.0057 and 0.0083 min^{-1} respectively. The amount of hydrogen generated from different catalysts was determined to be in the following order: powdery > network > fiber.

Keywords: TiO_2; Network geometry; Fiber geometry; Methyl orange; Photocatalytic activity; Hydrogen generation

1. Introduction

Homogeneous photocatalysis using semiconducting oxide catalysts has recently emerged as an efficient method for purifying water and also air and hydrogen generation [1–3].

TiO_2 is the most effective semiconductor used in clean energy and water treatment applications because of its great properties and several advantages such as high photochemical stability, low cost, non-toxicity and availability [2,4].

Most studies dealing with photocatalytic degradation of pollutants and hydrogen generation by water-splitting applied in slurry form into the aqueous phase [5–7]. Employing powder suspensions is accompanied by three major problems: (1) the difficulty of separating inactive catalysts, (2) the difficulty of applying

*Corresponding author.

them to continuous flow systems, and (3) the tendency of the particle catalysts to aggregate [1,3,8].

Filtration, coagulation, flocculation or centrifugation are the different methods applied to achieve a catalyst-free solution and recycle the catalyst [3,9]. These methods require the implementation of a post-treatment recovery step, which would significantly increase treatment cost and time [10,11]. This problem has resulted in development of several kinds of immobilization techniques to immobilize the photocatalyst powder, which may reduce the post-treatment expenses and time [1,8,12]. One way to make an immobile photocatalyst is to produce multi-dimensional structures such as thin-film, nanotube, nanowire, fiber, network, etc. which are fixed to the walls of the reaction reactor [2,3].

Various photocatalyst particle supports such as alumina, zeolite, silica gel, fiber optic cable, glass beads, quartz, stainless steels, clays and activated carbon have been investigated [3,13]. Of the various geometries, network structure, which is a hollow three-dimensional structure, has the potential for producing a new class of materials with novel applications. This structure is very important for practical applications because its pores have potentially large surface-to-volume ratios providing a significant advantage in the diffusion pathways which can be used as a kind of host for organic pollutants [2].

In the present study, the photocatalytic activity of fiber and network geometry of TiO_2 on methyl orange (MeO) decolorization, and hydrogen evolution from water-methanol mixture under ultra-violet (UV) light irradiation were investigated. Catalysts were characterized by XRD, SEM and Brunauer–Emmett–Teller (BET) and also compared for their catalytic behavior.

2. Experimental

Titanium tetraisopropoxide (TTIP), hydrochloric acid (HCl), 2-propanol and methyl orange (MeO) were purchased from MERCK manufacturer. Distilled water, cellulose fibers and ceramic templates were obtained from local sources. After thorough mixing, titanium isopropoxide (5 mL) was gradually added to the solution by a pipette. When the solution became clear, its temperature was elevated to 60˚C by immersing its container into a water bath. The substrates (cellulose fiber or ceramic templates) were then dipped in to the solution and left overnight to allow precipitation of a TiO_2 layer. The sample was then washed with deionized water and dried. The sample was then calcined at 450˚C for 2 h.

Fig. 1(a) shows molecular structure of cellulose fiber describing hollow pores which could be employed for fabrication of fibers. Cotton fiber has more than 90% cellulose which by being heated at over 370˚C burns fast [14]. A microscopic view of cotton is shown in Fig. 1(b).

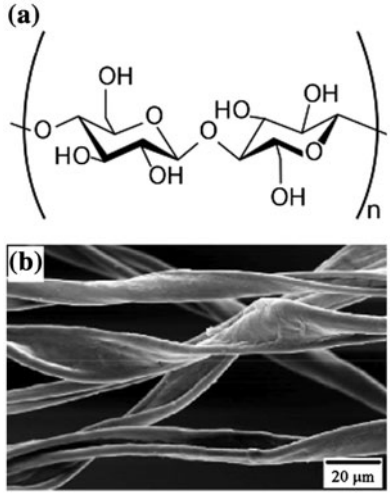

Fig. 1. (a) Molecular structure and (b) SEM image of cellulose fiber.

Fig. 2(a) is an image of ceramic template with pore size of 20 PPI, surface area of 2.0×10^4 cm^2/g and open porosity of 85–90% [14]. XRD pattern of the ceramic templates employed to manufacture network-shaped sample is represented in Fig. 2(b). All the peaks are related to the phase SiC and confirm the presence of this composition in the ceramic template.

2.1. TiO_2 characterization

X-ray diffractometer (Spectro Xepos, Germany) with Cu K_α radiation was used to determine the XRD patterns of the samples. SEM (Mira 3-XMU; Tescan, Czech Republic) was used for morphological investigation of the samples. Specific surface area of the produced samples was measured by using a BET surface analyzer (Belsorp mini II; Bel, Japan).

2.2. Photocatalytic degradation

Catalytic activity of the samples was estimated from color degradation of the methyl orange aqueous solution (50 mL MeO with 5 mg/L initial concentration). The pH was maintained constant and it was initial pH (6.5) of the MeO solution. The same amount of catalyst was used. Before irradiation with UV light, the aqueous solution which contained TiO_2 catalyst was continuously stirred for 1 h in full darkness to achieve adsorption–desorption equilibrium. UV irradiation from two 6 W lamp (Philips, China) was then

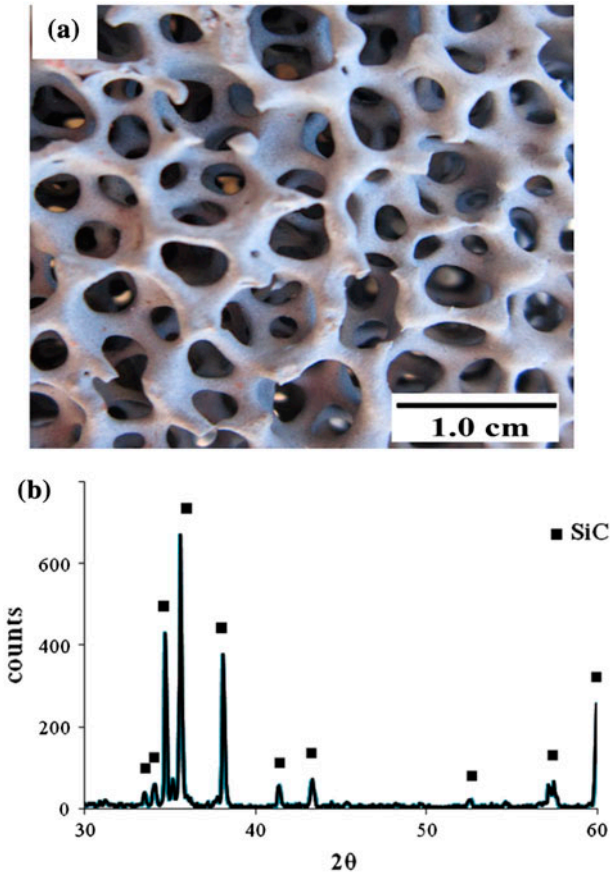

Fig. 2. (a) A shape and (b) XRD pattern of the ceramic templates.

applied to the catalyst containing solution. The distance between the surface of the solution and the light source was 10 cm. Samples were then taken out for analysis, every 30 min.

Solution concentration was determined by UV–vis spectrophotometer (6705; Jenway, UK). The maximum absorption wavelength registered of MeO was 462 nm. The efficiency of degradation ($\eta\%$) was calculated from the Eq. (1) [4,15]:

$$\eta\% = \left(\frac{C_0 - C}{C_0}\right) \times 100 \quad (1)$$

where C_0 and C are initial and time dependant concentrations of the dye, respectively.

2.3. Hydrogen generation

For methanol/water (50:50) photo-splitting, same amount of a photocatalyst was added to 200 mL distilled water in a 750 mL Pyrex reactor. UV-lamps (3×6 W/cm^2 = 18 W/cm^2, Philips) were used. Methanol/water photo-splitting was carried out for 2 h with constant stirring, and the level of hydrogen evolution was measured at 30 min intervals. The hydrogen gas (H_2) produced was analyzed by TCD-type gas chromatography (GC, model 2550TG; Islamic Republic of Iran).

3. Result and discussion

XRD pattern of TiO_2 is shown in Fig. 3. This spectrum belongs to TiO_2 particles existing in network and fiber geometries calcined at 450˚C for two hours. Based on the peaks of this pattern, anatase and rutile are the only phases present in the sample. The XRD pattern shows a crystalline structure of the anatase phase due to the existence of the distinguished peaks at 2θ of about 25.4˚, 37.8˚, 48.0˚, and 53.7˚, which correspond to the indices of (1 0 1), (1 0 3), (2 0 0), and (1 0 5) diffraction planes of the anatase TiO_2 respectively. Also, the existence of the distinguished peaks at 2θ of about 27.5˚, 36.1˚, 49.2˚, and 44.0˚, which correspond to the indices of (1 1 0), (1 0 1), (1 1 1), and (2 1 0) diffraction planes respectively, indicates the formation of the rutile TiO_2 [7]. Using the Scherer Equation, the average crystallite sizes of anatase and rutile were estimated to be 19 and 21 nm respectively.

The fraction of the crystalline phases was determined by integrating the relative intensities of the anatase (1 0 1) (2θ = 25.4˚) and the rutile (1 1 0) (2θ = 27.5˚) peaks [16]:

$$W_A = \frac{1}{1 + 1.26\frac{I_R}{I_A}} \quad (2)$$

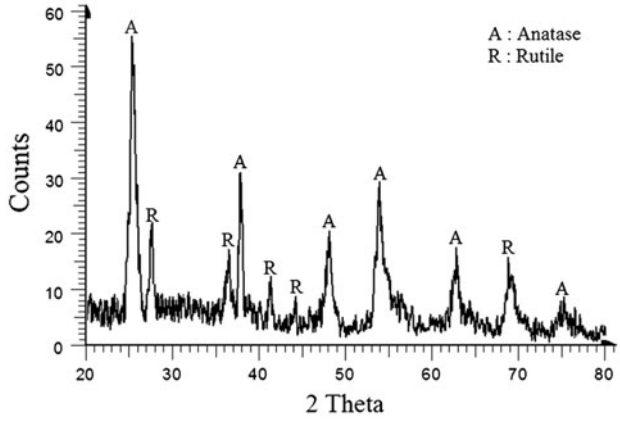

Fig. 3. XRD pattern of TiO_2 powder used in geometries calcined at 450˚C for 2 h.

where W_A is the weight fraction of the anatase and I_A and I_R represent the integrated intensities of the anatase (1 0 1) and the rutile (1 1 0) peaks respectively. With the aid of Eq. (2), the amount of anatase phase for the sample calcined at 450°C was calculated to be 73%.

SEM images of TiO_2 samples produced in this research are shown in Figs. 4 and 5. Fig. 4 indicates SEM images of TiO_2 microfibers under different levels of magnifications. Fig. 4(a) and (b) shows how fiber structure is formed after being heated and cotton fiber being removed. At a higher level of magnification a large number of finer fibers are observable in every tubular-shaped mass. TiO_2 microfibers are 30 μm long hollow cylinders having diameters of 0.5–1 μm.

Energy dispersive X-ray (EDS) analysis of the fibers shown in Fig. 4(c) indicated Ti and O presence in the annealed samples. Therefore, calcination at 450°C for 2 h led to the removal of all the cellulose of the template.

From XRD and EDS results, all cotton fibers left the structure completely at 450°C. This is why this temperature was decided upon for calcinations of network structure too.

Fig. 5(a) illustrates the layer of TiO_2 deposited on the surface of ceramic substrate. The morphology of the layer was homogeneous and appears almost spherical particles, with presence of porous forming a high porosity surface, which can enhance the catalytic activity of the geometry. The particles of which this layer is composed are roughly 30–60 nm in size.

According to Fig. 5(b), this deposited layer has a thickness of less than 10 μm. The layer thickness is proportional to the substrate holding time in the solution. The thickness will increase if the holding time increases. By studying the EDS diagram in Fig. 5(c), according to the SiC substrate, only two elements of oxygen and titanium are detected on the surface.

One of the vital factors in analyzing the properties of catalysts different geometries is studying their specific surface areas. The specific surface areas of samples which were used in this research are also listed in Table 1. In the coated sample (network), due to agglomeration of the particles, and the placement of particles on one another and also on the substrate, the surface area decreased (58.1 m^2/g) in comparison to the powdery sample. In fact, the surface area of the catalyst is minimized since the coating layer has a lower porosity. Due to the accumulation of fibers and closure of some of them, the surface area of the fiber sample is greatly reduced (from 68.2 m^2/g in powder to 48.7 m^2/g in fiber).

The absorption phenomenon under presence of TiO_2 geometries was investigated in the dark for MeO having the initial concentration of 5 mg/L, catalyst concentration of 150 mg/L and the constant pH 6.5. Adsorption kinetics obtained and shown in Fig. 6(a) indicates that the thermodynamic equilibrium time was 60 min. To study the kinetics of adsorption in its totality, the Lagergren model [17] given by the following equation was used:

$$q_t = q_e[1 - \exp(-k_{ads}t)] \quad (3)$$

where q_t and q_e (mg/g) are the adsorbed amount at t instant and at equilibrium respectively, k_{ads} is the apparent kinetic constant (1/min). The adsorption kinetics was well fitted as first order with this model. Enhancement of both MeO equilibrium adsorbed amount and the apparent constant k_{ads} which can be correlated with the increase of surface area of TiO_2 geometry as already mentioned. Moreover, powdery catalyst exhibits the high BET surface area which may provide more active sites for the photocatalytic reaction.

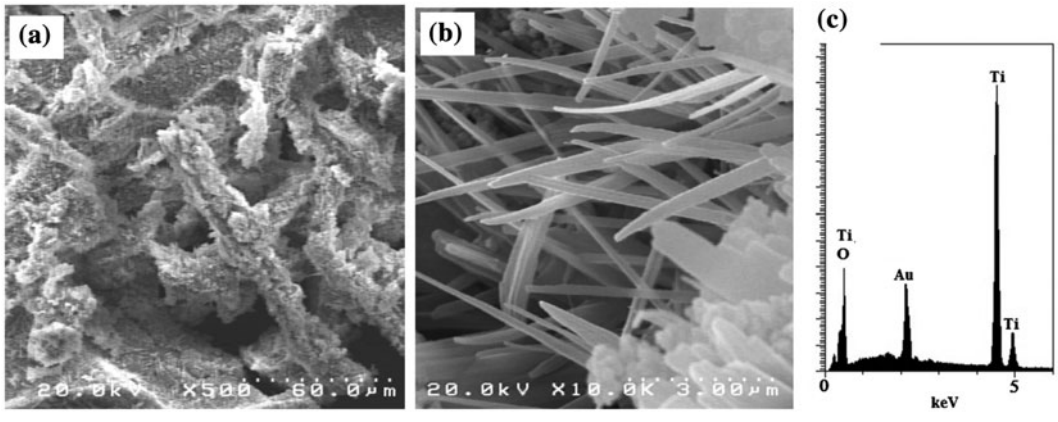

Fig. 4. TiO_2 fiber: (a) and (b) SEM image and (c) EDS diagram of fibers.

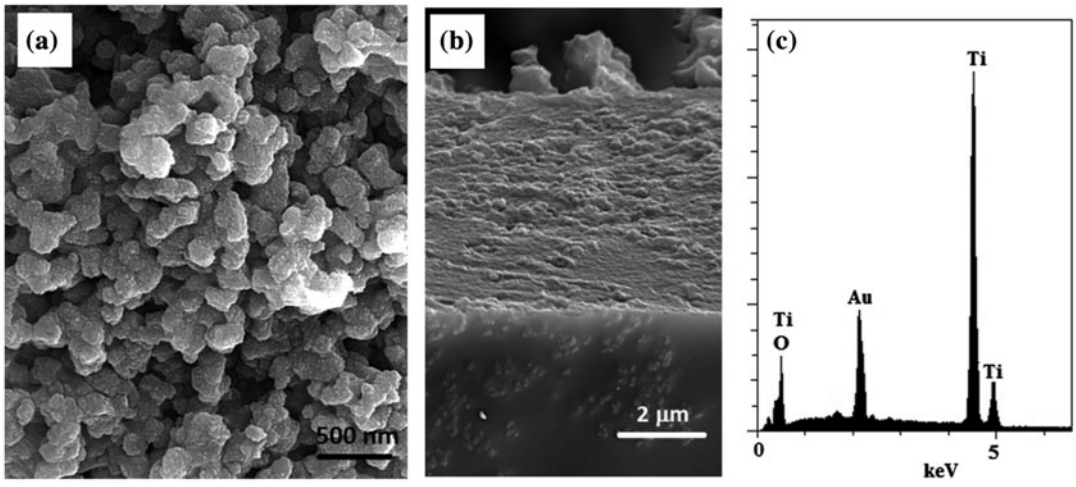

Fig. 5. TiO_2 network sample: (a) SEM image, (b) cross section image and (c) EDS diagram.

Table 1
Surface area and kinetic parameters for MeO degradation of various geometries

		Methyl orange	
Sample	S_{BET} (m^2/g)	K (1/min)	R^2
Powder	68.2	0.0118	0.989
Network	58.1	0.0083	0.997
Fiber	48.7	0.0057	0.991

The photocatalytic activity of TiO_2 powder was evaluated by using the degradation of the standard organic dye, methyl orange, under UV–vis light irradiation. The results displayed in Fig. 6(b) show the bands relating to different molecular parts in this dye are decreased with respect to time.

The degradation experiments by UV irradiation of methyl orange aqueous solutions containing TiO_2 photocatalyst follow the pseudo-first-order kinetics with respect to the concentration of the dyestuff in the bulk solution (C) [4,18]:

$$-\frac{dC}{dt} = k_{app} C \tag{4}$$

Integration of that equation (with the same restriction of $C = C_0$ at $t = 0$, with C_0 being the initial concentration in the bulk solution after dark adsorption and t the reaction time) will lead to the expected relation:

$$\ln\left(\frac{C_0}{C}\right) = k_{app} t \tag{5}$$

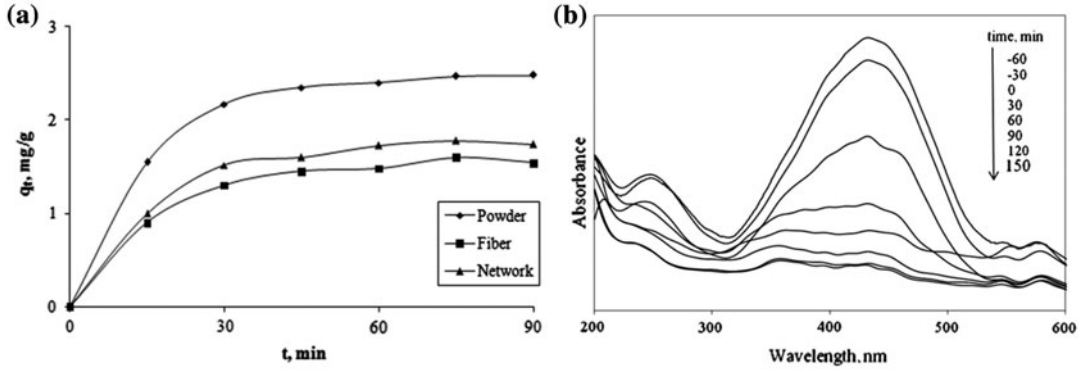

Fig. 6. (a) Adsorption kinetics of MeO on TiO_2 geometries in the dark and (b) changes in the UV–vis spectra during photodegradation of methyl orange on TiO_2 powder.

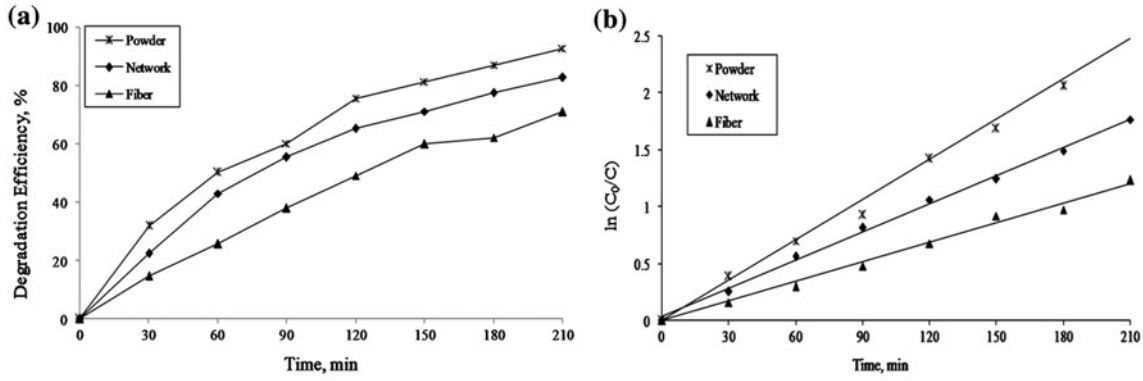

Fig. 7. (a) First order kinetic plots and (b) degradation efficiency of the MeO photodegradation in presence of different catalysts.

in which k_{app} is the apparent pseudo-first-order rate constant and is affected by dyestuff concentration [18].

The plot of $\ln(C_0/C)$ vs. time was close to linear for all the experiments (Fig. 7(a)). Same initial concentrations (5 mg/L) of MeO were used to obtain data of Fig. 7(a). Degradation rate constant (k_{app}) of the MeO dye is listed in Table 1. The effect of TiO_2 fibers and network on the efficiency of the MeO degradation is shown in Fig. 7(b). By examining the results, it is evident that the network structure, compared to fibers, has a greater efficiency of decolorization. The cause of that may lie in the network structure's larger specific surface area with respect to that of fiber. In this case, the contact area of the solution with the photocatalyst increases and so does the rate of dye degradation reactions.

Release degree (RD) factor examination was designed to analyze the degree to which TiO_2 particles are released from the substrate into the water while water treatment. In this examination, a specific amount of photocatalyst was put in pure water and after stirring it for a certain period of time, the density of photocatalyst released into water was determined. RD of the prepared geometries in pure water was determined by UV–vis spectrophotometer.

Powdery catalyst with 100% RD moves with the solution and cannot be removed from the reaction environment easily. After 60 min, fiber and network structures have RD of 48 and 9% respectively. Hence network geometry is the most suitable shape of TiO_2 catalyst; it has all the advantages of production simplicity, environmental stability, and high catalytic performance.

One of today's main industrial wastewater treatment strategies is focused on the development of green technologies and management practices for the environmental benefit. Then, catalyst recycling can be

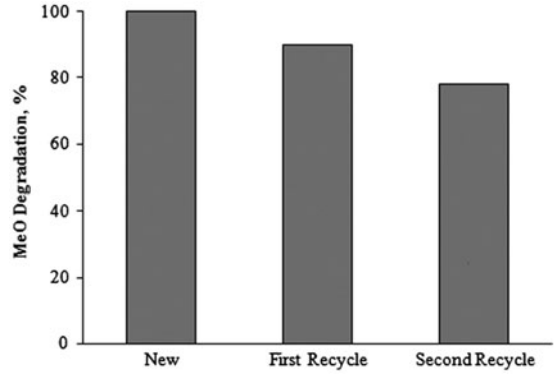

Fig. 8. Effect of network catalyst recycling on the photocatalytic degradation of MeO under 60 min of irradiation duration (initial MeO concentration = 5 mg/L).

foreseen as a good practice for sustainable wastewater treatment. Consequently, it is necessary to demonstrate whether, after a photocatalytic treatment, the catalyst can be reused.

The results of the degradation reaction using fresh immobilized network geometry, and once- or twice-recycled network geometry are shown in Fig. 8. There were slight decreases in photocatalytic efficiencies of the network geometry in the second and third cycles. The loss in the percentage of photocatalytic degradation was less than 30% even after the third cycle. After each experimental run, the photocatalytic activity of the network geometry decreases due to the fact that TiO_2 particles move into the solution and active sites get blocked by some MeO intermediates.

The activities for photocatalytic hydrogen production over different geometries of TiO_2 have been investigated and the results are shown in Fig. 9. A much higher hydrogen generation was achieved in the range of 693 μmol/h over powdery photocatalyst, as it

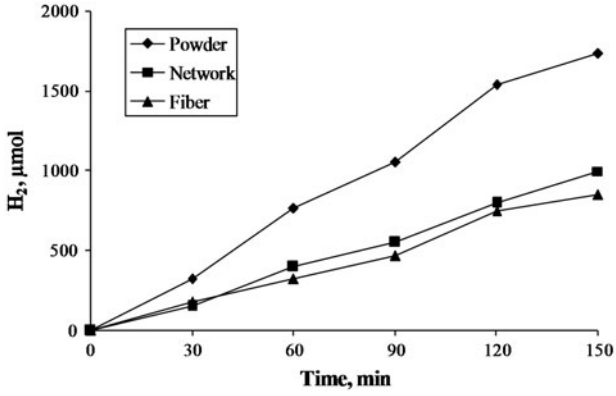

Fig. 9. Effect of TiO_2 geometry on H_2 generation activity from 50 vol.% methanol solution.

is dependent on the preparation process. As having been stated in decolorization experiment, considering the higher specific level of this sample than those of network and fiber, this result was predicted. The other two samples, their specific surface area being low, yielded less hydrogen. Here too, just like the decolorization experiment, their photocatalytic activities were not the same, but here the difference in the two structures photocatalytic performances was subtle.

4. Conclusions

In this research, fiber and network geometry of TiO_2 were obtained by precipitation on the substrate. Their different properties were investigated by various analyses. To determine the photocatalytic activity, dye degradation and hydrogen generation experiments were carried out. TiO_2 powder with the specific surface area of 68.2 m^2/g had the highest efficiency in decolorizing and hydrogen generating. Network geometry having a larger specific surface area compared to that of fiber geometry indicated a higher efficiency in photocatalytic performance.

References

[1] M. Shahid, A. McDonagh, J.H. Kim, H.K. Shon, Magnetised titanium dioxide (TiO_2) for water purification: Preparation, characterisation and application, Desalin. Water Treat. 54 (2015) 979–1002.
[2] H. Koohestani, S.K. Sadrnezhad, Photocatalytic activity of immobilized geometries of TiO_2, J. Mater. Eng. Perform. 24 (2015) 2757–2763.
[3] N. Alenzi, W.S. Liao, P.S. Cremer, V.S. Torres, T.K. Wood, C.E. Economides, Z. Cheng, Photoelectrochemical hydrogen production from water/methanol decomposition using Ag/TiO_2 nanocomposite thin films, Int. J. Hydrogen Energy 35 (2010) 11768–11775.
[4] A.H. Jawad, A.F.M. Alkarkhi, N.S.A. Mubarak, Photocatalytic decolorization of methylene blue by an immobilized TiO_2 film under visible light irradiation: Optimization using response surface methodology (RSM), Desalin. Water Treat. 2014 (2014) 1–12.
[5] V. Koutantou, M. Kostadima, E. Chatzisymeon, Z. Frontistis, V. Binas, D. Venieri, D. Mantzavinos, Solar photocatalytic decomposition of estrogens over immobilized zinc oxide, Catal. Today 209 (2013) 66–73.
[6] A. Kudo, Y. Miseki, Heterogeneous photocatalyst materials for water splitting, Chem. Soc. Rev. 38 (2009) 253–278.
[7] S. Onsuratoom, S. Chavadej, T. Sreethawong, Hydrogen production from water splitting under UV light irradiation over Ag-loaded mesoporous-assembled TiO_2-ZrO_2 mixed oxide nanocrystal photocatalysts, Int. J. Hydrogen Energy 36 (2011) 5246–5261.
[8] I.M. Arabatzis, T. Stergiopoulos, M.C. Bernard, D. Labou, S.G. Neophytides, P. Falaras, Silver-modified titanium dioxide thin films for efficient photodegradation of methyl orange, Appl. Catal. B: Environ. 42 (2003) 187–201.
[9] A. Haenel, P. Moren, A. Zaleska, J. Hupka, Photocatalytic activity of TiO_2 immobilized on glass beads, Physicochem. Probl. Miner. Process 45 (2010) 49–56.
[10] G. Veréb, Z. Ambrus, Z. Pap, K. Mogyorósi, A. Dombi, K. Hernádi, Immobilization of crystallized photocatalysts on ceramic paper by titanium(IV) ethoxide and photocatalytic decomposition of phenol, React. Kinet. Mech. Catal. 113 (2014) 293–303.
[11] S.Z. Kang, Z. Gu, D. Gu, J. Mu, Immobilization and photocatalytic activity of TiO_2 nanoparticles on porous aluminium foil, J. Dispersion Sci. Technol. 26 (2005) 169–171.
[12] D. Mukherjee, S. Barghi, A.K. Ray, Preparation and characterization of the TiO_2 immobilized polymeric photocatalyst for degradation of aspirin under UV and solar light, Processes 2 (2013) 12–23.
[13] R. Leary, A. Westwood, Carbonaceous nanomaterials for the enhancement of TiO_2 photocatalysis, Carbon 49 (2011) 741–772.
[14] J. Militky, Structure and Properties of Cotton Fiber: A Literature, Review 2009, Dr Muhammad Mushtaq Mangat, 1–51.
[15] N. Laoufi, D. Tassalit, F. Bentahar, The degradation of phenol in water solution by TiO_2 photocatalysis in a helical reactor, Global NEST J. 10 (2008) 404–418.
[16] M. Mazaheri, Z.R. Hesabi, S.K. Sadrnezhaad, Two-step sintering of titania nanoceramics assisted by anatase-to-rutile phase transformation, Scr. Mater. 59 (2008) 139–142.
[17] Y. Kang, X. Li, Y. Tu, Q. Wang, H. Ågren, On the mechanism of protein adsorption onto hydroxylated and nonhydroxylated TiO_2 surfaces, J. Phys. Chem. C 114 (2010) 14496–14502.
[18] F.A. Babakhani, A.R. Mehrabadi, P.N.L. Lens, M. Sadatian, Prevention of biofilm formation in water and wastewater installations by application of TiO_2 nano particles coating, Desalin. Water Treat. 28 (2011) 83–87.